

Determination of solution aggregation using solubility, conductivity, calorimetry, and pH measurements

William H. Streng*, Daniel H.-S. Yu, Chengyue Zhu

Hoechst Marion Roussel, Inc., P.O. Box 9627, Kansas City, MO 64134, USA

Received 26 April 1995; revised 9 September 1995; accepted 11 September 1995

Abstract

Compounds which aggregate or form micelles have an unusually high solubility and/or have a solubility which is very sensitive to temperature. Theoretical equations are derived which relate the data collected from conductivity and calorimetric experiments to the average aggregation number, equilibrium constant, and the enthalpy change for the aggregation. For the compound studied, the amount of aggregation occurring was found to be small with an aggregation number of 10–11 and an equilibrium constant of 10^{10} – 10^{12} . The *cmc* is temperature dependent, having a value of 0.033 M at 15°C increasing to 0.045 M at 35°C. The aggregation is primarily enthalpy driven and entropy disfavored. The aggregated compound has a lower pK_a than the monomer, according to the pH data, indicating that the imidazole ring is less basic in the aggregate.

Keywords: Micelle formation; Aggregation; Solubility; Conductivity

1. Introduction

Synthetic organic compounds typically have aqueous solubilities less than 0.5 M at room temperature when their molecular weights are greater than 300. During the solution characterization of compound I (Fig. 1), it was observed that the solubility of I was greater than would be expected for a synthetic organic compound with no additional interactions in solution and that the solubility appeared to have a greater sensitivity to

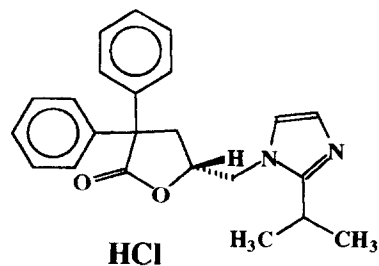


Fig. 1. Compound I. MDL 201,346A. (R)-2(3H)-furanone,dihydro-5-[[2-(1-methylethyl)-1H-imidazole-1-yl]methyl]-3,3-diphenyl-,hydrochloric salt.

* Corresponding author.

temperature than expected. It is well known that this solubility behavior is indicative of aggregation or micelle formation (Attwood and Florence, 1983).

It was, therefore, of interest to determine the solubility/temperature profile of I in water over the temperature range 2.5–35°C and to determine the critical micelle concentration (*cmc*), average aggregation number (*n*), and equilibrium constant (K_m) for the observed aggregation using conductivity, calorimetry, and pH measurements.

2. Theoretical section

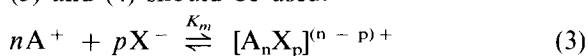
The formation of a micelle by singly-charged monomers can be expressed as the equilibrium in Eq. (1), with the formation constant given by Eq. (2).



$$K_m = \frac{\gamma_M}{(\gamma_A)^n} \cdot \frac{c_M}{(c_T - nc_M)^n} \quad (2)$$

where: A^+ represents the monomer; $(A_n)^{n+}$ represents the micelle; *n* = aggregation number; K_m = equilibrium constant; γ_M = micelle activity coefficient; γ_A = monomer activity coefficient; c_T = total concentration of the compound; c_M = equilibrium micelle concentration.

If the counterion is involved in the micelle, Eqs. (3) and (4) should be used.



$$K_m = \frac{\gamma_M}{(\gamma_A)^n(\gamma_X)^p} \cdot \frac{c_M}{(c_T - nc_M)^n(c_T - pc_M)^p} \quad (4)$$

where: X^- represents the counteranion; *p* = number of anions in a micelle; γ_X = counteranion activity coefficient.

The formation of micelles in a solution is expected to cause changes in certain physical properties such as surface tension, osmotic pressure, light scattering, conductivity (Preston, 1948), pH, and heat of dilution (Anderson et al., 1975). Since the concentration of micelles at equilibrium is critically dependent upon the total concentration of the compound, important information with regard to the *cmc*, *n*, and K_m can be obtained

from the profiles of certain physical chemical properties vs. total concentration of the compound.

Since micelle formation in a solution can be rather complicated and involves multiple equilibria and a wide range of micelle sizes, an accurate description and evaluation of all the parameters for the system may become difficult and impractical. However, it has been reported that the sizes of micelles in a solution follow a certain pattern of distribution and the majority of micelles fall into a fairly narrow size range (Tanford, 1973). Therefore, the modeling of the system may be simplified by considering only one type of micelle formed with a single aggregation number. The aggregation number should not be too different from the average aggregation number in the real system.

In addition to this single micelle type assumption, three other assumptions were also introduced in modeling the following conductivity and calorimetric data:

- (1) The micelles are formed from the singly-charged, protonated form of the compound. Based on its pK_a (7.82¹), compound I should remain mostly protonated at the solution pH of these studies.
- (2) The activity coefficients for all the species involved in the micelle formation are assumed to be constant and close to unity. For the association of charged species, the activity coefficients of the reactants and the products were found to cancel to a large degree (Ghosh and Mukerjee, 1970).
- (3) The counterions (chloride in this case) are not an integral part of the micelles and their involvement were not pursued. Chloride ions are highly solvated in aqueous solution and it is unlikely that chloride ions will become an integral part of the micelles, especially if the micelles are small.

¹ The value 7.82 was obtained from the pH concentration data following. A potentiometric titration resulted in a value of 6.82.

2.1. Conductivity data treatment

Since the micelle and the monomer should have significantly different charges and mobilities, the formation of micelles should affect the overall electrical conductivity of the solution. Therefore, conductivity measurements as a function of concentration should provide important information as to whether or not micelles are formed. As shown below, it is possible to determine the *cmc* value, the *n* number, and K_m from the conductivity data.

Consider the monomer and the micelle as two distinct electrolytes, the total conductivity (κ) of a solution containing both monomers and micelles will be:

$$\kappa = \kappa_A + \kappa_M \quad (5)$$

where: κ_A = monomer conductivity; κ_M = micelle conductivity.

Rewriting Eq. (5) in terms of molar conductivity (Λ) results in:

$$\Lambda = \frac{\kappa}{c_T} = \frac{c_A}{c_T} \Lambda_A + \frac{c_M}{c_T} \Lambda_M = \frac{(c_T - nc_M)}{c_M} \Lambda_A + \frac{c_M}{c_T} \Lambda_M \quad (6)$$

where: Λ = total molar conductivity; Λ_A = molar conductivity of the monomer; Λ_M = molar conductivity of the micelle.

Further, consider both the monomer and the micelle as strong electrolytes; Λ_A and Λ_M can then be expressed as linear functions of the square roots of c_A and c_M , respectively, according to Onsager theory (Moore, 1972). Therefore, Eq. (6) can be rewritten as:

$$\Lambda = \frac{(c_T - nc_M)}{c_T} (a - b \sqrt{c_T - nc_M}) + \frac{c_M}{c_T} (a' - b' \sqrt{c_M}) \quad (7)$$

where: a = limiting molar conductivity (molar conductivity at infinite dilution) of monomer; b = a constant for the monomer; a' = limiting molar conductivity of micelle; b' = a constant for the micelle.

At concentrations well below the *cmc*, $c_M = 0$ and Eq. (7) reduces to $\Lambda = a - b\sqrt{c_T}$. The constants a and b can be obtained by fitting conductivity data over the low concentration range. The same approach cannot be applied to obtain a' and b' since it is not correct to assume $c_A = 0$ over the high concentration range. Therefore, a' and b' must be obtained as two independent parameters. In Eq. (7), c_M is a function of K_m and n , as defined by Eq. (2). Theoretically, values of K_m , n , a' , and b' can be obtained by fitting the experimental $\Lambda_{obs,i}$ vs. $\sqrt{c_{T,i}}$ data using a non-linear least-squares regression method. During the regression process, the value of F , Eq. (8), is minimized. The equations used in the data fitting were Eq. (2) (or Eq. (4)), Eqs. (7) and (8).

$$F(K_m, n, a', b') = \sum_{i=1}^{NP} \left(\frac{\Lambda_{obs,i} - \Lambda_{cal,i}}{\Lambda_{cal,i}} \right)^2 \quad (8)$$

where: NP = number of data points; $\Lambda_{obs,i}$ = observed total molar conductivity; $\Lambda_{cal,i}$ = calculated total molar conductivity.

2.2. Calorimetric data treatment

Since micelles are present in solution in significant amounts only when the total concentration of the monomer exceeds the *cmc*, dilution of the solution to a concentration well below the *cmc* should result in complete dissociation of the micelles. The heat effect associated with this process should provide a measure of the concentration of the micelles present in the original solution.

Heat of dilution measurements were carried out using an isoperibol titration calorimeter. In a heat of dilution experiment, a known amount of sample solution is delivered into the bulk solvent through a continuous titration and the heat effect associated with the dilution is measured. For a solution containing micelles, the total heat of dilution is a sum of heats from micelle dissociation, proton dissociation, dilution of micelles, and dilution of monomers:

$$\begin{aligned} Q_{Net} &= Q_{Diss,M} + Q_{Diss,H} + Q_{Dil,M} + Q_{Dil,A} \\ &= \Delta n_{Diss,M} \Delta H_{Diss,M} + \Delta n_{Diss,H} \Delta H_{Diss,H} \\ &\quad + \Delta n_M \Delta H_{Dil,M} + \Delta n_A \Delta H_{Dil,A} \end{aligned} \quad (9)$$

where: $Q_{Diss,M}$ = heat of micelle dissociation; $Q_{Diss,H}$ = heat of proton dissociation; $Q_{Dil,M}$ = heat of dilution for micelle; $Q_{Dil,A}$ = heat of dilution for monomer; $\Delta n_{Diss,M}$ = number of moles of micelle dissociated due to the dilution; $\Delta n_{Diss,H}$ = number of moles of proton dissociated due to the dilution; Δn_M = number of moles of micelle diluted; Δn_A = number of moles of monomer diluted.

If the pK_a of the compound is sufficiently high (e.g. ≥ 6.0) and the concentration of the compound after dilution is not too low (e.g. $\geq 10^{-4}$ M but $\ll cmc$), the pH of the solution will remain sufficiently low such that the compound will remain mostly protonated during the dilution process and the heat effect associated with the proton dissociation should be negligible. Therefore, Eq. (9) can be reduced to:

$$Q_{Net} \approx Q_{Diss,M} + Q_{Dil,M} + Q_{Dil,A} \approx \Delta n_{Diss,M} \Delta H_{Diss,M} + \Delta n_M \Delta H_{Dil,M} + \Delta n_A \Delta H_{Dil,A} \quad (10)$$

Dividing Q_{Net} by the total number of moles of compound diluted gives the apparent molar heat of dilution $-\phi_L$. By assuming complete micelle dissociation after dilution, $-\phi_L$ can be expressed as:

$$-\phi_L \approx c_M \frac{\Delta H_{Diss,M}}{c_T} + c_M \frac{\Delta H_{Dil,M}}{c_T} + c_A \frac{\Delta H_{Dil,A}}{c_T} \quad (11)$$

where: c_M = equilibrium concentration of micelle in titrant; c_A = equilibrium concentration of monomer in titrant; c_T = total concentration of the compound in titrant.

According to Eq. (11), in order to obtain $\Delta H_{Diss,M}$, values of $\Delta H_{Dil,M}$ and $\Delta H_{Dil,A}$ must be known. This requirement is rather difficult to fulfil since direct measurement of $\Delta H_{Dil,M}$ is not always possible. As an approximation, it is assumed first that the heat of dilution for the monomer is negligible and second, $\Delta H_{Dil,M}/(nc_M)$ is a constant (where n is the aggregation number for the micelle). Applying the two assumptions to Eq. (11) leads to Eq. (12):

$$-\phi_L \approx \frac{c_M}{c_T} \Delta H_{Diss,M} + \frac{(nc_M)c_M}{c_T} \Delta H_{DL} \quad (12)$$

where: $\Delta H_{DL} = \Delta H_{Dil,M}/(nc_M)$.

ΔH_{DL} can be estimated from the $-\phi_L$ vs. c_T profile at the high concentration region and considered a known constant in Eq. (12).

Combining Eqs. (2) and (12), the unknown parameters n , K_m , and $\Delta H_{Diss,M}$ ($\Delta H_{Diss,M} = -\Delta H_m$) can be obtained by fitting the experimental $-\phi_L$ vs. c_T data using a non-linear least squares procedure.

3. Experimental section

3.1. Solubility measurements

An excess amount of compound I was placed into a Wheaton flint glass ampoule. Five milliliters of water were added and the ampoule placed in a Lauda RM6 constant temperature bath ($\pm 0.1^\circ\text{C}$) at the desired temperature. The ampoule was removed from the bath and then heat sealed and transferred to a Tamson TEV 45 constant temperature bath ($\pm 0.01^\circ\text{C}$) and allowed to equilibrate with agitation (Vibro Mixer E1, Chemapec Inc.) for at least 2 days.

After equilibration, the ampoule was removed from the constant temperature bath and the supernatant was immediately removed and diluted with the HPLC mobile phase. Further dilution with the mobile phase was made to prepare the samples for the HPLC assay. Each sample was assayed in triplicate by HPLC and the solubility was determined.

The procedure was repeated for each temperature. For the samples above ambient temperature, i.e. 25, 30, and 35°C , the sample preparation after equilibration was performed in an environmental chamber set to the temperature of the study to prevent cooling of the sample.

HPLC assay:

(1) Instruments:

- (a) Alcott 728 autosampler (64 position tray)
- (b) Kratos Spectroflow 783 absorbance detector
- (c) Waters chromatography pump

- (d) Spherisorb ODS-2 HPLC column, $5\mu\text{m}$, $250 \times 4.6\text{ mm}$.
- (2) Mobile phase: 60:40 (v/v) of acetonitrile/0.025 M KH_2PO_4 aqueous solution.
- (3) Conditions:
- Flow rate: 1 ml/min
 - Wavelength: 220 nm
 - Temperature: ambient
 - Sample size: 20 μl
 - Data acquisition: PeakPro, supplied by Beckman Instruments.

Standard solutions of I with concentrations from 6.25 $\mu\text{g/ml}$ to 50 $\mu\text{g/ml}$ were prepared. The entire set of standard solutions was injected at the beginning and the end of the HPLC run, and selected standards were injected throughout the run after approximately every nine samples. The median area response of each standard solution was fit to the following expression:

$$y = ax^b \quad (13)$$

where: y = concentration; x = peak area; a , b = parameters to be determined by fitting the equation using standard solutions.

The concentration of each sample was determined according to its peak area and Eq. (13).

3.2. Density measurements

Solution densities of I were determined using a Mettler DA-310 temperature-controlled densitometer. To avoid precipitation during density measurements, the densities of the 95% saturated solutions were measured. The measured density data were fit to the equation $\text{density} = m \times \text{concentration} + b$, where m and b are constants. The densities for the saturated solutions were then calculated using this equation.

3.3. Conductivity measurements

The RadioMeter conductivity cell used in this study was calibrated using a 0.100 M potassium chloride aqueous solution at 15, 25, and 35°C. The experimental procedure for the conductivity measurements of I was as follows. In a 40-ml glass test tube, 20.0 ml of I (ca. 0.2 M) was added.

The solution was stirred with a magnetic stirrer and was equilibrated (Lauda RM6 constant temperature bath) at the study temperature. The conductivity of this solution was measured using a RadioMeter CDC 304 conductivity cell and a RadioMeter CDM83 conductivity meter. Either a 1.0-ml or a 2.0-ml aliquot of this solution was removed from the test tube and replaced with exactly the same amount of water. The resulting solution was stirred and equilibrated, and the conductivity of this diluted solution was measured. Successive dilution and conductivity measurements were continued until the concentration of the last diluted solution was about 0.01 M. In order to obtain a constant conductivity reading, the solutions were equilibrated for 15–20 min.

3.4. pH measurement

The pH values for the solutions of I with concentrations ranging from 0.01 M to 0.23 M were measured at 25°C using a RadioMeter GK2401 glass electrode and a RadioMeter PHM85 pH meter.

3.5. Heat of dilution measurements

The heats of dilution of I at 25°C were determined calorimetrically using a Tronac isoperibol (temperature-rise) titration calorimeter. In each heat of dilution experiment, about 1.6 ml of an aqueous solution of I was delivered into 25 ml water in a 25-ml reaction vessel through continuous titration. The reaction vessel was positioned inside a high-precision controlled water bath (controlled to $\pm 0.0005^\circ\text{C}$ using a Tronac temperature controller PTC-41) set at the desired temperature (known to $\pm 0.01^\circ\text{C}$) and was in thermal equilibrium with its surroundings before the start of titration. The solution inside the reaction vessel was efficiently stirred during the experiment and the temperature of the solution was continuously monitored by a high-sensitivity thermister and recorded every 10 s, thus resulting in a temperature vs. time profile. The temperature vs. time profile was then converted to the reaction heat vs. time (dilution heat vs. time, in this case) profile, the thermogram, after making all the corrections

Table 1
Solubility of I in water and solution density at different temperatures

Temperature °C	Solubility (mg/ml)	Solubility (molarity)	Solution density ^a (g/ml)
2.5	12.5	0.0315	1.00229
5.0	14.5	0.0365	1.00280
7.5	18.9	0.0476	1.00342
10.0	25.3	0.0637	1.00415
15.0	154	0.388	1.02988
20.0	241	0.607	1.04112
25.0	396	0.998	1.06789
30.0	467	1.177	1.07278
35.0	521	1.313	1.08271

^aDensities of 95% saturated solutions.

for non-reaction heats. A heater calibration run was conducted before and after the titration run to provide the necessary calibration parameters for the conversion. The theory of calorimeter calibration and heat corrections have been described elsewhere (Hansen et al., 1985).

Heat of dilution measurements were performed on a series of solution concentrations of I ranging from 0.01 M to 0.23 M. From each titration experiment, a thermogram showing the heat of dilution as a function of time (or as a function of compound concentration after dilution, i.e. the compound concentration in the reaction vessel) was obtained. The apparent molar heat of dilution, $-\phi_L$, for a given solution of I which was diluted to a given lower ('after-dilution' or 'diluting-to') concentration was determined from the thermogram by dividing the observed heat of dilution at the given 'after-dilution' concentration by the number of moles of compound diluted at this point. The given 'diluting-to' concentration was 0.001 M for all the heat of dilution measurements.

The calorimeter operation and data acquisition were controlled using software developed in house. A HP 3421A data acquisition control unit, a custom-made junction box, a National Instruments GPIB PCIIA interface board, and National Instruments NI 488.2 handler software were used to interface the Tronac 1250 calorimeter with a personal computer.

4. Results and discussion

Table 1 and Fig. 2 show the solubility/temperature profile of I in water. The solubility is greater than 10 mg/ml for all the temperatures studied with a dramatic increase above 10°C.

As described previously (Lewis and Randall, 1961), the solubility and temperature of regular solutions can be related by the following equation:

$$\frac{\partial (\ln x_2)}{\partial (1/T)} = -\frac{\Delta\bar{H}}{R} \quad (14)$$

where: x_2 = the solubility of the solute expressed in mole fraction; $\Delta\bar{H}$ = the differential heat of solution; R = the gas constant, 8.3143 J K⁻¹ mol⁻¹, and T = the absolute temperature of the solution. $\Delta\bar{H}$ can be obtained by plotting \ln

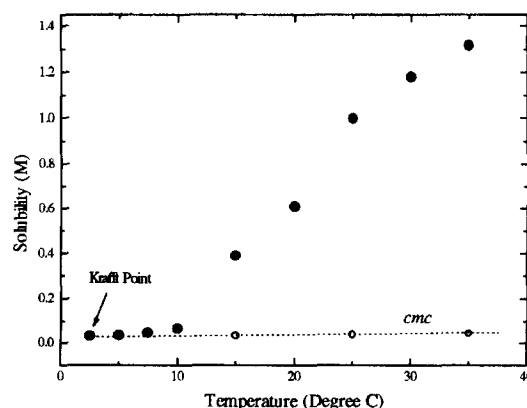


Fig. 2. Solubility vs. temperature profile for I in water.

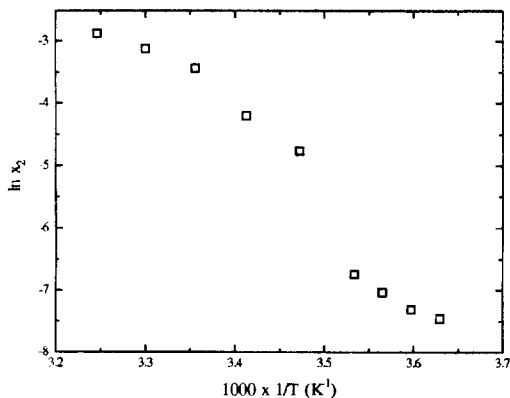


Fig. 3. Relation between $\ln x_2$ and $1/T$ for saturated solutions of I.

x_2 vs. $1/T$, where x_2 can be obtained from the solubility and density of the saturated solution at each temperature.

According to Fig. 3 there is not a linear relationship between $\ln x_2$ and $1/T$, as predicted in Eq. (14), and, therefore, I in water is not behaving as a regular solution. The dramatic increase in solubility of I as the temperature increases resembles that for many detergent solutions (Shinoda and Hutchinson, 1962) which form micelles and have dramatic physical property changes close to their 'critical micelle concentration'.

Fig. 4 shows the molar conductivity vs. square root of concentration for I in water at 25°C. A

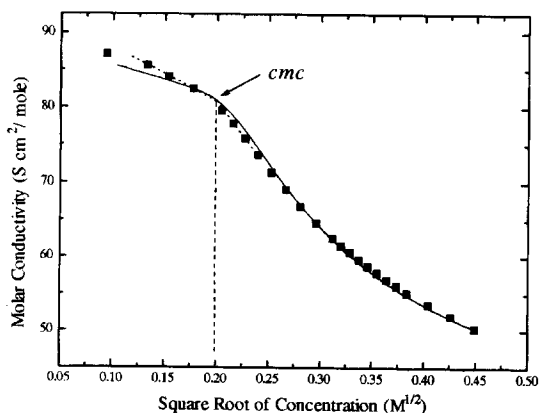


Fig. 4. Molar conductivity vs. square root of concentration profile (■, expt.; —, calcd.) for I in water at 25°C.

Table 2
Values of 'cmc' for I in water at different temperatures

Temp. (°C)	cmc (M)	
	From conductivity	From heat of dilution
15	0.033	
25	0.040	0.038
35	0.045	

significant slope change at about $0.2 \text{ M}^{1/2}$ is seen in this profile. Since I is a strong electrolyte in aqueous solution, based on the Onsager theory (Moore, 1972), the Λ vs. $(c_T)^{1/2}$ profile of I should be approximately linear if no significant aggregation or micellization occurs within the concentration range studied. The apparent departure from linearity in the Λ vs. $(c_T)^{1/2}$ profile strongly suggests that significant self-association of I has occurred, especially at concentrations greater than 0.040 M . The cmc value for I in water at 25°C was thus estimated to be 0.040 M . Similar slope changes were also observed in the Λ vs. $(c_T)^{1/2}$ profiles at 15 and 35°C and the cmc values for I at these temperatures were also estimated (Table 2). As seen in Table 2, the cmc increases slightly as the temperature increases.

It is of interest to notice that the observed solubilities of I at temperatures below 10°C are comparable to or greater than the corresponding

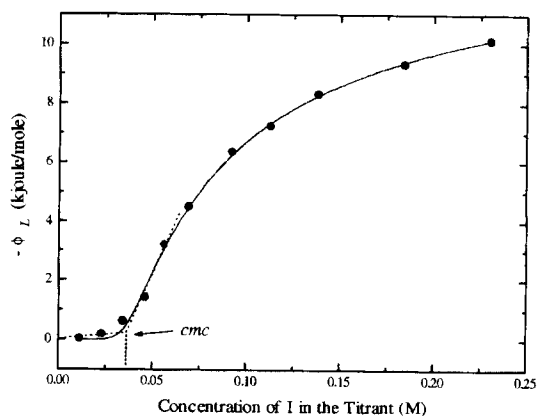


Fig. 5. $-\phi_L$ vs. concentration profile (●, expt.; —, calcd.) for I in water at 25°C.

Table 3
Parameters obtained by fitting the conductivity/concentration data for I in water at 25°C

Parameter	Value
n	10
$\log K_m$	10
a	89.5
b	38.9
a'	368
b'	46
F_{min}	0.031

cmc values (Fig. 5). This indicates that self-association also exists for I at temperatures below 10°C, but to a much smaller degree. According to theory (Shinoda and Hutchinson, 1962), the formation of micelles of large aggregation number (100 or greater) should result in a sharp solubility increase at the 'Krafft point', the temperature when the cmc equals the solubility. The lack of a dramatic solubility increase at the Krafft point (ca. 2.5°C, Fig. 2) suggests that the aggregation products formed by I are not very large. The fact that the observed inflection points in the A vs. $(c_T)^{1/2}$ profiles are not very sharp also supports this conclusion.

Based on the equations described earlier, the average aggregation number n and formation constant K_m for the aggregates were determined through regression analysis of the A vs. $(c_T)^{1/2}$ data. Excellent fit of the observed A vs. $(c_T)^{1/2}$ profile at 25°C (Fig. 4) was achieved using the parameters listed in Table 3. The n and K_m values for I at 25°C were found to be 10 and 10^{10} , respectively. The n number of 10 confirmed the expectation that the aggregates were not large, while the K_m value of 10^{10} , which is equivalent to a 5.7-kJ free energy decrease per mole of monomer, indicates that the driving force for the aggregate formation is rather significant.

It was also found from the conductivity study that the limiting molar conductivity for the aggregate, a' , was much greater than that for the corresponding monomer, a . This is understandable since the aggregate is highly charged as compared to the singly-charged monomer.

The presence of a cmc for I in water was also confirmed by having observed a definite inflection point in the heat of dilution vs. concentration profile for I at 25°C (Fig. 5). The cmc value found from these data agrees well with that found using the conductivity data at 25°C.

Excellent fit of the observed heat of dilution vs. concentration profile for I at 25°C (Fig. 4) was also achieved through regression analysis and the values of n , K_m , and ΔH_m (enthalpy of aggregation) were determined (Table 4). The entropy of aggregation ΔS_m (Table 4) was calculated according to the relation $-RT \ln K_m = \Delta H_m - T \Delta S_m$.

The values of n and K_m obtained from the heat of dilution data are in good agreement with those found using the conductivity data. The ΔH_m value of -142 kJ/mol of aggregate (12.9 kJ/mol of monomer) indicates that the aggregation of I is a strong exothermic reaction and is strongly favored enthalpically. Thermal energy is approximately 2.5 kJ/mol and therefore the energy available from thermal motion is not sufficient to break up the aggregate. Hydrogen bond energies are in the range of 8–32 kJ/mol which indicates that the aggregation can be attributed to hydrogen bonding. More specifically, C–H···O and N–H···O hydrogen bonds have energies in the range 8–12 kJ/mol which is in agreement with the enthalpy per monomer unit found experimentally. The ΔS_m value of -244 J K⁻¹ mol⁻¹ indicates that the process is entropically disfavored. This is understandable since the formation of an aggregate increases the order by bringing 'free' monomers together and forming an organized structure. It is concluded that the formation of aggregates by I in aqueous solution is purely enthalpy driven.

Table 4
Parameters obtained by fitting the heat of dilution/concentration data for I in water at 25°C

Parameter	Value
n	11
$\log K_m$	12.1
ΔG_m (kJ mol ⁻¹)	-69.1
ΔH_m (kJ mol ⁻¹)	-142
ΔS_m (J K ⁻¹ mol ⁻¹)	-244
F_{min}	0.0367

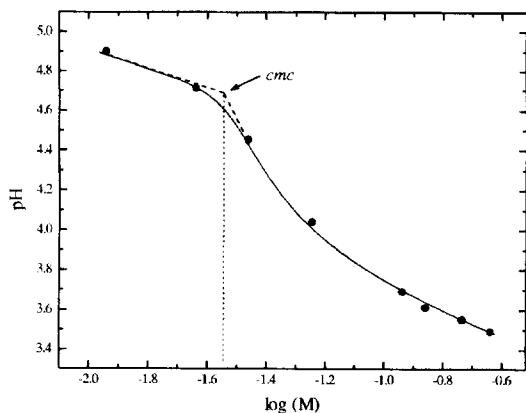


Fig. 6. pH vs. logarithm of concentration profile (●, expt.; ----, calcd.) for I in Water at 25°C.

In performing the calculations, the assumption was made with both the conductivity and calorimetric studies that the sizes of the aggregates fell into a narrow range and that the average aggregation number is a constant over the concentration range studied. From the excellent fit of the experimental data with the calculated curves (Figs. 4 and 5), it can be concluded that the assumptions are reasonable. It would be unlikely that a good fit could be made over the entire concentration range if the size range were wide. If this occurred, the average aggregation number would be expected to change as the concentration changed. Also, the small molar heat of dilution for solution concentrations less than the *cmc* confirms the assumption that the heat of dilution for the monomer is negligible. Furthermore, since the solution pH is less than 5.0 and the pK_a is between 7 and 8 for the monomer, the heat effect due to a change in the concentration of the protonated species should be negligible.

Finally, the evidence for aggregation was also found in the pH vs. log M profile for I at 25°C (Fig. 6) which displayed a large slope change at ca. 0.029 M. A function can be written which relates the pK_a s for the monomer and the aggregate to the pH and total concentration. It can be shown that the slope of the curve in Fig. 6 should equal 0.5 when there is no aggregation.

Deviation of this slope from 0.5 can be attributed to aggregation. Calculation of the pK_a values using these data result in values of 7.82 for the monomer and 6.25 for the aggregate. It has been shown (Preston, 1948) that the observed *cmc* value can vary using different physical chemical properties. The values obtained for the *cmc* from conductivity and calorimetric measurements are upper limits while the value obtained from pH measurements is a lower limit. The important information provided by the pH vs. log M profile is that the pK_a for the aggregate is less than the monomer and therefore the aggregation results in making the imidazole ring a weaker base. Because there is an effect upon the pK_a , the stabilizing energy of 12.9 kJ/mol of monomer discussed earlier might involve the imidazole ring in the form of N–H···O hydrogen bonding, or it might be due to structural effects in which the individual molecules are sufficiently close to cause the imidazole ring to be less basic due to intramolecular charge effects.

5. Conclusions

Compound I was found to undergo significant aggregation in water at temperatures higher than 10°C and concentrations greater than the *cmc*'s. Evidence for aggregation include: (1) a sharp solubility increase at 10°C in the solubility vs. temperature profile; (2) a significant slope change in the molar conductivity vs. square root of concentration profiles at 15, 25 and 35°C; (3) a clear inflection point in the heat of dilution vs. concentration profile at 25°C; and (4) a significant change in slope in the pH vs. log M profile at 25°C.

The *cmc* for I in water at 25°C is approximately 0.04 M. The average aggregation number n for I at 25°C is ca. 10–11, which represents small-sized micelles or aggregates. The average formation constant K_m for the aggregates in water at 25°C is ca. 10^{10} – 10^{12} . The formation of aggregates by I in water is enthalpy driven and entropy disfavored.

Acknowledgements

We want to thank Scott Peterson for his assistance in conducting the experiments.

References

- Anderson, B.D., Rytting, J.H., Lindenbaum, S. and Higuchi, T., *J. Phys. Chem.*, 79 (1975) 2340–2344.
- Attwood, D. and Florence, A.T., *Surfactant Systems, Their Chemistry, Pharmacy and Biology*, Chapman and Hall, New York, 1983, pp. 44–46.
- Ghosh, A.K. and Mukerjee, P., Multiple association equilibria in the self-association of methylene blue and other dyes. *J. Am. Chem. Soc.*, 92 (1970) 6408–6410.
- Hansen, L.D., Lewis, E.A. and Eatough, D.J., Instrumentation and data reduction. In Grime, K. (Ed.), *Analytical Solution Calorimetry*, Ch. 3, Wiley, New York, 1985, pp. 57–95.
- Lewis, G.N. and Randall, M., revised by Pitzer, K.S. and Brewer, L., *Thermodynamics*, 2nd Edn., McGraw-Hill, New York, 1961, p. 228.
- Moore, W.J., *Physical Chemistry*, Longman, London, 1972, pp. 425, 457–458.
- Preston, W.C., Some correlating principles of detergent solutions. *J. Phys. Colloid Chem.*, 52 (1948) 84–97.
- Shinoda, K. and Hutchinson, E., Pseudo-phase separation model for thermodynamic calculations on micellar solutions. *J. Phys. Chem.*, 66 (1962) 577–582.
- Tanford, C., *The Hydrophobic Effect: Formation of Micelles and Biological Membranes*, Wiley, New York, 1973, pp. 60–70.